Chitosan-g-PMMA/Kaolin Bionanocomposites for Use in Bioadhesive Bone-Cement Implants

Arun Kumar Pradhan[1,2]*, Prafulla Kumar Sahoo[1] and Pradeep Kumar Rana[2]

[1]*Department of Chemistry, Utkal University, Vani Vihar, Bhubaneswar 751 004, India*
[2]*Plastics and Polymer Engineering Department, Maharashtra Institute of Technology, Aurangabad, Maharashtra 431005, India*

Received October 19, 2016; Accepted March 14, 2017

ABSTRACT: Chitosan grafted with poly(methyl-methacrylate) (PMMA) and adsorbed with kaolin functionalized as bioadhesive was prepared via emulsion polymerization technique and physiochemically characterized as a bone-graft substitute. The so prepared grafted bioactive bone cement (BBC) bionanocomposites (BNCs), chitosan-g-PMMA/kaolin, was characterized by Fourier transform infrared (FTIR) spectroscopy, X-ray diffraction (XRD) analysis, field-emission scanning electron microscopy (FESEM) and thermogravimetric analysis (TGA). The water uptake, retention ability and the nanosize particle arrangement in the polymeric BBC-BNCs were studied along with the mechanical and biodegradation properties. These preliminary investigations of the BNCs will open the door for their use in bioadhesive bone-cement implants in the future.

KEYWORDS: Chitosan, bone cement, bionanocomposite, bioadhesive

1 INTRODUCTION

Bone cements must possess proper injectability, a quick setting time, suitable modulus bioactivity, a low setting temperature, and radiopacity. Even if small-scale bone fractures can be easily self-repaired, large-scale bone defects (i.e., comminuted fracture, osteoporotic and cartilaginous tissues) are difficult to self-heal via regeneration and remodeling [1]. In this case, repeated surgery is necessary to insert a bone graft or artificial materials at the site of the defect [2]. According to reported information, there are more than 2 million operations requiring bone substitutes each year in the United States and other parts of the world, and the demand continues to rise drastically. The traditional bone repair procedure involves the use of autografts (from the patient's iliac crest) and allografts (from the cadaver bone) [3]. Previously, an autograft was considered the gold standard in the reconstruction of bone defects because it has structural stability and natural osteogenic ability [4, 5].

Although the autograft and allograft procedures have been fairly successful, there are serious limitations such as limited supply of donor bone tissue, unpredictable rejection characteristics, and infection [3, 6]. Large bone defects in particular are a major clinical problem since autologous bone grafts are not available in up to 40% of these patients [7]. Therefore, there is a pressing need for more reliable and abundant bone substitutes to replace or repair bone by filling the defect with either PMMA or bioabsorbable ceramic bone graft substitutes in cement defects in clinics.

Individually, PMMA has not gained wide acceptance when used for fracture treatment in the extremities because of its inability to remodel and possibly inhibit fracture healing [8].

Among the many potential bone cement materials, PMMA or its derivatives has been used successfully in orthopedic surgeries. PMMA was first introduced as bone cement in the early 1960s by Charnley and Smith [9]. It conforms to the shape of its surroundings, allows even distribution of implant loads, and forms a strong mechanical bond with implants. However, its widespread use is limited by several complications. For example, PMMA adheres insufficiently to bone surfaces (no bioactivity) [10]. It is weaker than cortical bone [11], has a high exothermic reaction temperature [12, 13], and exhibits monomer toxicity [14].

To address concerns regarding PMMA and modified PMMA, several investigations of different bioactive bone cements (BBCs) have been conducted with the addition of hydroxyapatite (HA) powder [15].

*Corresponding author: akpradhanchem@gmail.com

DOI: 10.7569/JRM.2017.634129

Other researchers have added bone particles and growth hormones to PMMA cement [16, 17]. Another potential additive is chitosan, which is biodegradable, soluble in organic acid solutions and resistant to alkali environments. Chitosan is a copolymer of glucosamine and N-acetylglucosamine deacetylated from the natural polymer chitin. Chitosan also has a high resistance to heat due to its intramolecular hydrogen bonds [18]. Chitosan-based PMMA composite exhibits biological properties such as biodegradability, biocompatibility, and immunological and antibacterial activities. Although improvements have been realized, many fundamental problems with PMMA remain unresolved. The purpose of this study was to develop novel BBC, composed of kaolin and chitosan, for use in orthopedic surgeries such as vertebroplasty or as bone filler.

2 MATERIAL AND METHODS

2.1 Materials

The deacetylated chitosan and initiator, ammonium persulfate, were purchased from HiMedia, Mumbai, India. The methyl methacrylate (MMA) and kaolin were from SRL Ltd., India, and sorbitol from Qualigen, India Ltd.

2.1.1 Deacetylation of Chitosan

To increase the amine content of chitosan, chitosan with a 76% degree of deacetylation was further deacetylated according to the modified procedure to increase the degree of deacetylation to above 90%. Degree of deacetylation or $\%NH_2$ group is determined by potentiometric titration method as per the report [19] described below. The degree of deacetylation (DD) of the chitosan sample was prepared by adding 0.14 g chitosan into 35 mL NaCl solution (0.1 mol/L) and then adding 14 ml HCl (0.106 mol/L) of the standard solution to achieve protonation, thus increasing its solubility. The pH value was adjusted to 6 by adding NaOH (0.01 mol/L) of the standard solution and calculating the total volume of NaOH solution consumed for the other replicates and then adding 0.3 mL cellulase solution (160 U/mL). After incubation for 6 h in a 40 °C water bath, the chitosan solution was taken out and replenished with HCl solution and the pH was adjusted back to about 2.5. By adding NaCl the total volume was maintained at about 50 ml. With the aid of the pH meter, chitosan was titrated with NaOH and then after the two immediate pH changes (pH > 10.5), retitrated with HCl solution, bringing the pH back to < 3. This process involves two abrupt pH changes and both the pH values and the consumption of NaOH (or HCl) are recorded. The DD is calculated by using the following formula [19]:

$$DD = \frac{203.195 \times W(NH_2)}{16.02262 + 0.42037 \times W(NH_2)} \quad (1)$$

$$W(NH_2) = \frac{V \times C \times 100 \times 0.016}{Wdry}$$

where V, C and $Wdry$ stand for volume of NaOH (or HCl) consumption between two abrupt changes of pH, concentration of NaOH (or HCl), and the dry weight of chitosan sample (derived from the moisture content) respectively. DD and $W(NH_2)$ are based on the percentage.

2.1.2 Preparation of Chitosan-g-PMMA Graft Copolymer and Chitosan-g-PMMA/Kaolin Graft Composite

To make the grafted composite, i.e., chitosan-g-PMMA (BBC1), chitosan (0.25 gm), monomer (MMA), initiator amonium persulphate (APS) along with complex catalyst $CuSO_4$ and glycine (1:1) and surfactant sorbitol (0.05 gm) were added sequentially to the reaction vessels. Then a different set of kaolin-based graft copolymer samples were prepared, taking the same quantity of monomer MMA and chitosan in the reaction vessels followed by addition of kaolin (BBC2 = 0.25%, BBC3 = 0.5%, BBC4 = 0.75%, BBC5 = 1.0% and BBC6 = 1.5%) to each vessel, as shown in Table 1. The mixtures were stirred overnight for 14 h for complete insertion of monomer into the chitosan at 25 °C. Under N_2 atmosphere the desired quantity of initiator APS, complex initiator $CuSO_4$ and glycine (1:1) along with the surfactant were added at 55 °C. Then the reaction was continued by stirring for 3 h and then stopped by quenching the vessel in ice water. The graft copolymer and the additive-based graft copolymer were washed three times with hot water and acetone and were oven dried at 70 °C for 3 h and kept in the desiccators for 1 h to make them moisture-free and then weighed. The material so prepared is shown in Scheme 1.

2.1.3 Calculation of Grafting Parameters

For chitosan copolymers, the grafting parameter was obtained by using the following expression:

$$\text{Yield of grafting (\%)} = [(\text{wt of graft copolymer} - \text{wt of chitosan})/\text{wt of chitosan}] \times 100 \quad (2)$$

Table 1 Variation of MMA and (%) of grafting.

Sample code	Chitosan gm	MMA ml	APS gm	$CuSO_4$ gm	Glycine gm	Sorbitol gm	Kaolin gm	% of Grafting
BBC1	0.25	3	0.684	0.32	0.15	0.05	–	89.6
BBC2	0.25	1	0.684	0.32	0.15	0.05	0.25	–
BBC3	0.25	2	0.684	0.32	0.15	0.05	0.5	–
BBC4	0.25	3	0.684	0.32	0.15	0.05	0.75	–
BBC5	0.25	4	0.684	0.32	0.15	0.05	1.0	–
BBC6	0.25	5	0.684	0.32	0.15	0.05	1.5	–

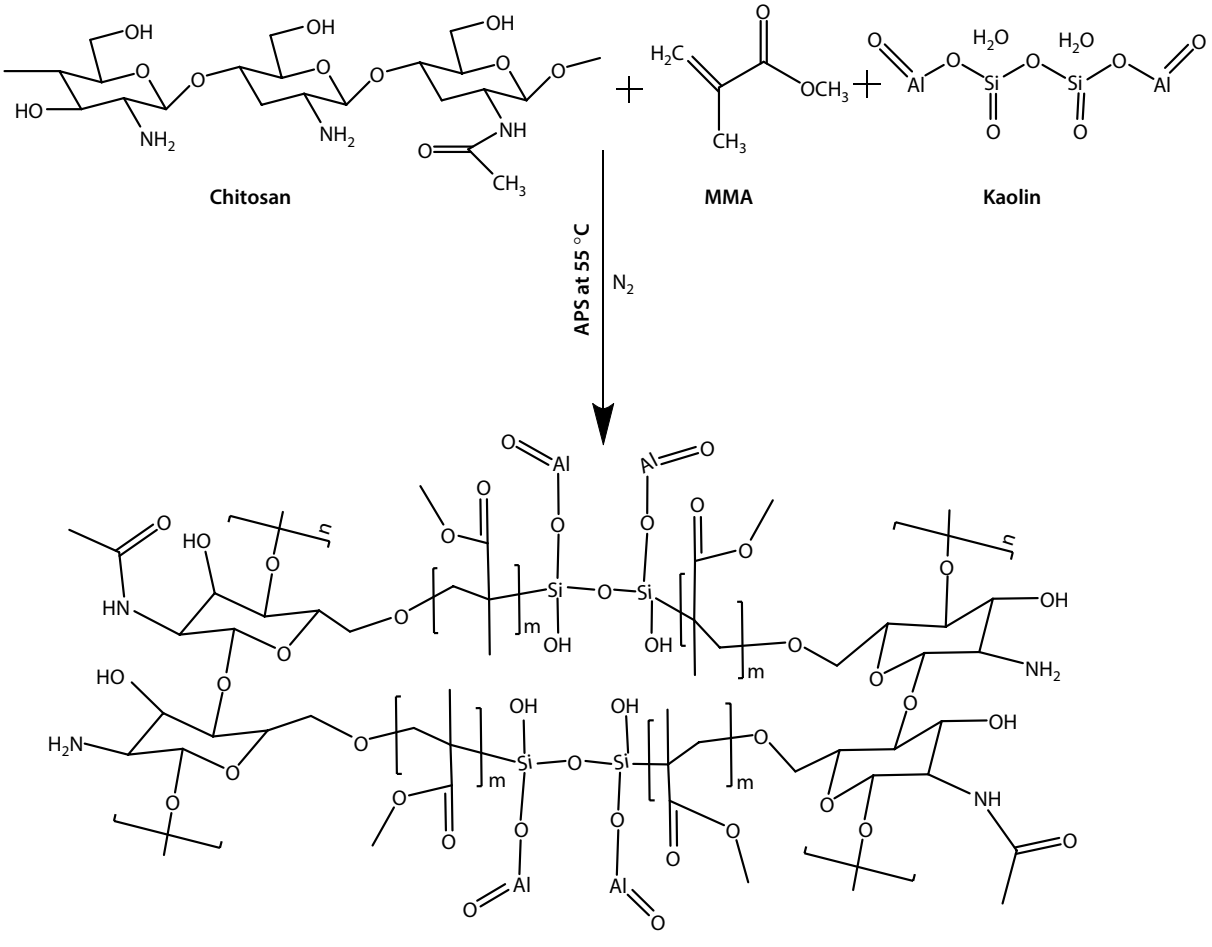

Scheme 1 Chitosan-g-PMMA/kaolin.

3 CHARACTERIZATION

The PMMA grafted chitosan sample and kaolin-based bionanocomposite BBCs were characterized by FTIR, XRD, FESEM and TGA. The insertion of PMMA into the chitosan was confirmed by using an XRD monitoring diffraction angle 2θ from 10° to 90° on a Philips PW-1847 X-ray crystallographic unit equipped with a Guinier focusing camera with CuKα radiation (λ = 0.15059 nm) with a 0.02 2θ step size and a 2 s count time. Nanoscale structure of grafted samples was investigated by means of a FESEM accelerating voltage of 5.00 kV. The ultrathin section (the edge of the sample sheet perpendicular to the compression mold) with a thickness of 1 μm and 200 nm was microtomed at −80 °C on a Zeiss Mevlin SEM Instrument (FESEM). Thermal properties were measured by using a Shimadzu DTA-500 system. It was carried out in air

 DOI: 10.7569/JRM.2017.634129

from room temperature to 600 °C at a heating rate of 10 °C/min. The IR spectra of samples, in the form of KBr pellets, were recorded with a PerkinElmer model Paragon-500 FTIR spectrophotometer.

4 PROPERTIES

4.1 Testing of Mechanical Properties

The prepared BBCs were pressed between two glass plates for 1 h. After the cement had hardened, it was pulled out of the plates and stored at room temperature. Specimens of 75 × 5 × 3 mm dimension were prepared for the tensile tests [20].

The tensile test and three-point bending test were performed on an Instron universal materials testing machine (Model 5544). The tensile test (according to ASTM D638-03) was conducted at a crosshead speed of 1 mm/min.

The BBCs were poured into the mold for the compression and bending test, and fixed with PTFE endplates and C-shape fixture for 4 h. After the bone cements were hardened, the endplate and C-shape fixture were removed and then the cylindrical test specimens were taken out for the compressive strength test. The compressive strength of each specimen was determined according to ISO 5883-2002 standard using the same universal testing machine, operating at a crosshead speed of 5 mm/min.

4.2 Equilibrium Water Content (EWC)

Equilibrium water content of BCC nanocomposite with different kaolin content was studied to evaluate the effect of kaolin content on the size stability of material. The EWC Wa of BCC-BNCs at time t was calculated using the following equation:

$$Wa\% = \frac{wt - wo}{wo} \times 100 \quad (3)$$

where wt and wo are the weights of sample at time t and the dry state at 23 °C, in that order.

4.3 Biodegradation by Activated Sludge

The activated sludge water was collected from domestic wastewater. The sludge water contains many different types of microorganisms (bacteria, fungi, yeast, etc.) which are accountable for the biodegradation of waste materials. The sludge was collected in a polypropylene container, which was filled absolutely and then fully closed [21]. Then, the wastewater was brought to the lab immediately. After settling for about 1 h, the total solid concentration was increased to around 5000 mg/L. The activated sludge water and a polymer sample (0.2 g) were incubated together in a sterilized vessel at room temperature (28 ± 2 °C) for 15 days, 1 month, 3 months and 6 months. Duplicate samples were removed at time intervals for biodegradation study via weight loss. Vessels containing polymer samples without sludge water were treated as controls.

5 RESULT AND DISCUSSION

5.1 FTIR Spectra of the BBC-BNCs

The grafting of PMMA onto chitosan was confirmed by the FTIR spectral study, as shown in Figure 1. Figure 1e of the BNC indicates the absorption peak of the carbonyl group of chitosan-g-PMMA/kaolin segments at 1700 cm^{-1} and the Si-O at 1060 cm^{-1} and 890 cm^{-1}. From Figure 1c it can be seen that the absorption peak of the PMMA segment in the copolymer appears at 3100 cm^{-1} due to C-H stretching frequency. The typical spectra for amide bands of pure chitosan are located at 1680 cm^{-1}, as shown in Figure 1b. On the other hand, the carbonyl absorption band of the chitosan-g-PMMA shifted to lower frequency at 1665 cm^{-1}, as shown in Figure 1d. The slight shifting of the peak to lower frequency might be due to the hydrogen bonding between the amino group of chitosan and the carbonyl group of the pendant graft.

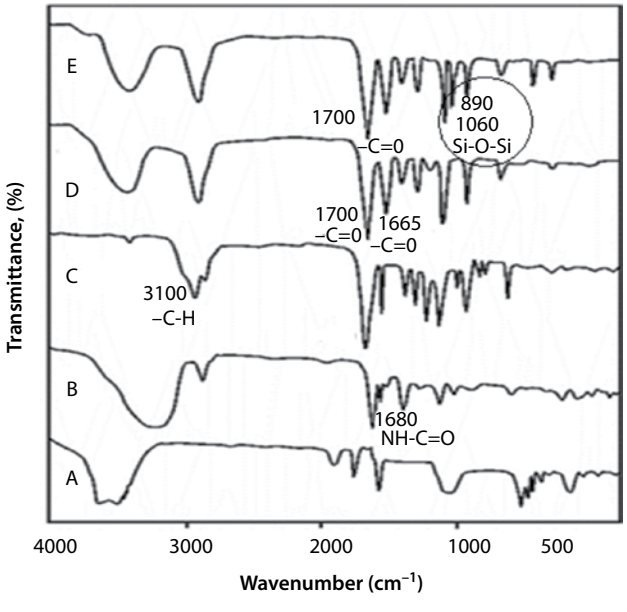

Figure 1 FTIR spectra of (**a**) kaolin, (**b**) chitosan, (**c**) PMMA, (**d**) chitosan-g-PMMA and (**e**) chitosan-g-PMMA/kaolin BNC.

5.2 XRD of the BBC-BNCs

The crystallinity of samples like kaolin, chitosan-g-PMMA (deacetylated) and chitosan-g-PMMA/kaolin were investigated by X-ray diffraction study. In the X-ray pattern in Figure 2a, the X-ray pattern of kaolin is showing sharp peaks due to its partially crystalline nature. But in the chitosan-g-PMMA in Figure 2b, the chitosan shows a broader pattern at around 2θ = 20°, indicating lower degree of crystallinity [22, 23]. It has been reported that the crystalline structure of chitin derivatives depends on the degree of deacetylation, i.e., the crystalline structure of shrimp chitosan is retained up to 70% of the deacetylation degree. But, upon further deacetylation, the crystalline regions of chitosan are destroyed and become amorphous. In Figure 2c, the chitosan-g-PMMA/kaolin sample confirms the insertion of polymer in the layered structure of kaolin. In the layered silicate structure the d-spacing of kaolin has been changed because the angle 2θ was changed between 13.2° and 24.3° in Figure 2a and 12.79° and 23.89° in Figure 2c. This clearly reveals the grafted polymer being introduced inside the layered silicate matrix of the kaolin.

5.3 FESEM of the BBC-BNCs

The FESEM micrographs of the copolymers without kaolin and with kaolin are shown in Figure 3 at different magnifications like 20 kX, 30 kX and 40 kX. The micrographs confirmed the homogeneous insertion of the graft copolymer into the matrix of the kaolin as comparatively shown in Figures 3a–c and d–f respectively. The surface morphology of chitosan-g-PMMA/kaolin BNC before biodegradation and after biodegradation (Figure 3g) was different, which indicated that the decomposition or colony growth of microorganisms in activated sludge has been confirmed on the chitosan-g-PMMA/kaolin BNC, resulting in the rough surface as compared to the surface prior to biodegradation. Hence, the prepared novel nanocomposite is eco-friendly in nature.

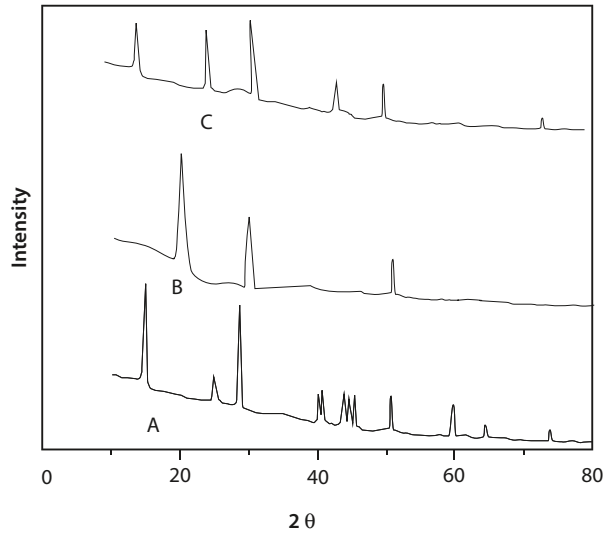

Figure 2 XRD of (**a**) kaolin, (**b**) chitosan-g-PMMA and (**c**) chitosan-g-PMMA/kaolin BNC.

5.4 TGA of the BBC-BNCs

The thermal decomposition of chitosan-g-PMMA and the first decomposition of chitosan-g-PMMA/kaolin were studied by TGA analysis, as shown in Figure 4. The initial decomposition of both the samples is due to the presence of a little bit of moisture in the samples; however, more moisture content is found in chitosan-g-PMMA/kaolin, showing the enhancement of hydrophilicity. Later, the decomposition of the chitosan-g-PMMA copolymer at temperature 155 °C and that of chitosan-g-PMMA/kaolin BNC at 258 °C is explained by the fact that the higher thermal decomposition of the BNC chitosan-g-PMMA/kaolin might be due to the insertion of the copolymer into the layered structures of the kaolin. This is an added advantage for this nanocomposite as it can resist the higher temperature.

5.5 Mechanical Properties of BBC-BNCs

The mechanical properties like tensile strength and compressive strength of the BNC samples were studied in freeze-dried condition for 48 h.

5.6 Tensile Strength

From the test results it has been observed that the tensile strength of the BBC-BNCs gradually increases from BBC1 to BBC4 and then decreases till BBC6. The increasing trend of the tensile strength might be ascribed to the gradual enhancement of the crosslinking of the PMMA with chitosan up to 44.3 MPa and after that the BBC-BNCs might become brittle due to higher crosslinking density; as a result, after 44.3 MPa there is a decreasing trend of tensile strength, as shown in Figure 5 [24].

5.7 Compressive Strength

The compressive strength results shown in Figure 5 are similar to that of tensile strength and the highest compressive strength found for BBC4 might be due to optimum crosslinking density. Here, from BBC1 to BBC4 there is an increase in compressive strength, i.e.,

 DOI: 10.7569/JRM.2017.634129

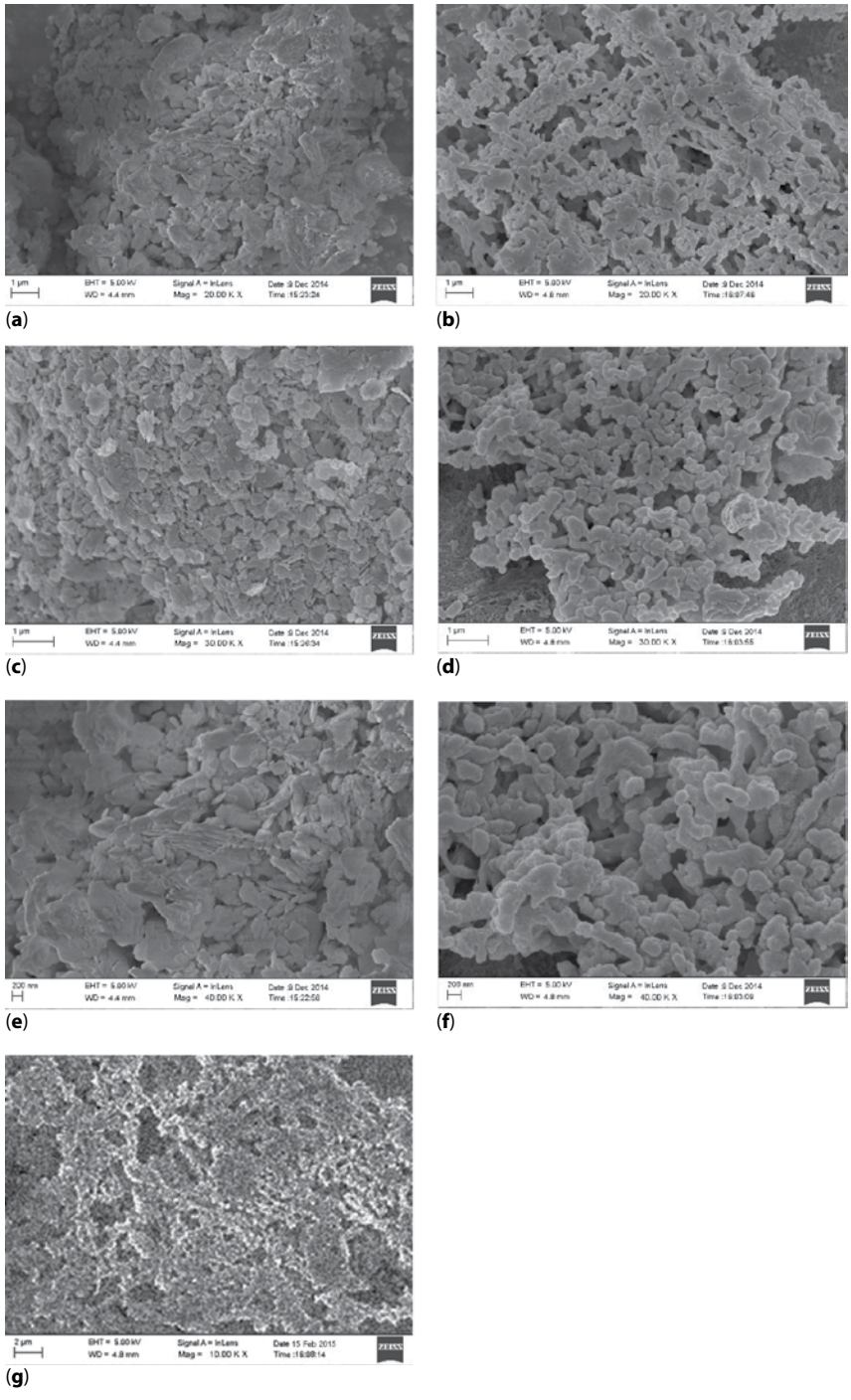

Figure 3 FESEM of (**a**) Chitosan-g-PMMA (**a**, **c** & **e**); (**b**) Chitosan-g-PMMA/kaolin (**b**, **d** & **f**); and (**c**) after biodegradation of Chitosan-g-PMMA/kaolin (**g**).

up to 54.9 Mpa; and after that it decreased up to sample BBC6, as shown in Figure 5 [25].

5.8 Equilibrium Water Content

The equilibrium water content depends on the amount of kaolin present in the BNC. The maximum percentage of water content is found in BBC2 due to getting more space in the composite matrix. After that, the sudden decrease in water absorbency up to BBC6 might be due to the increase in rigidity and crosslink density of the polymer inside the BNC. As a result, penetration and retaining capacity of the water might decrease.

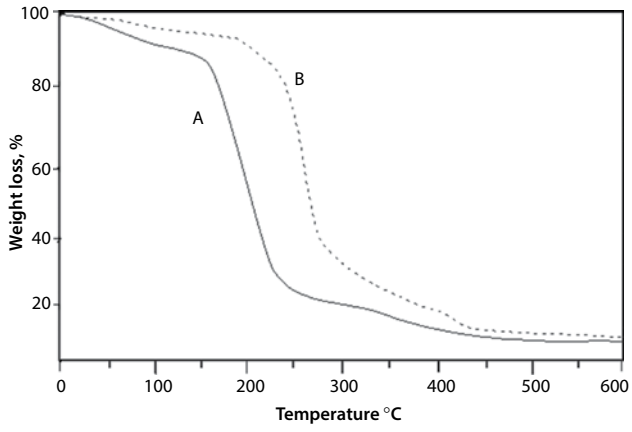

Figure 4 TGA thermograms of (**a**) chitosan-g-PMMA and (**b**) chitosan-g-PMMA/kaolin.

5.9 Biodegradation by Activated Sludge

From Figure 7 it is clear that from BBC1 to BBC4 there is an increasing trend of biodegradation compared to that of other BNCs. It might be ascribed to more water retention capacity of the BBC4 BNC; as a result, it might be giving microorganisms more of a chance to grow. For other BNCs, due to lower equilibrium water content, the biodegradation was found to be less.

6 CONCLUSION

The copolymer, chitosan-g-PMMA, and the BNC, chitosan-g-PMMA/kaolin, were synthesized via emulsion technique using APS as an initiator under N_2

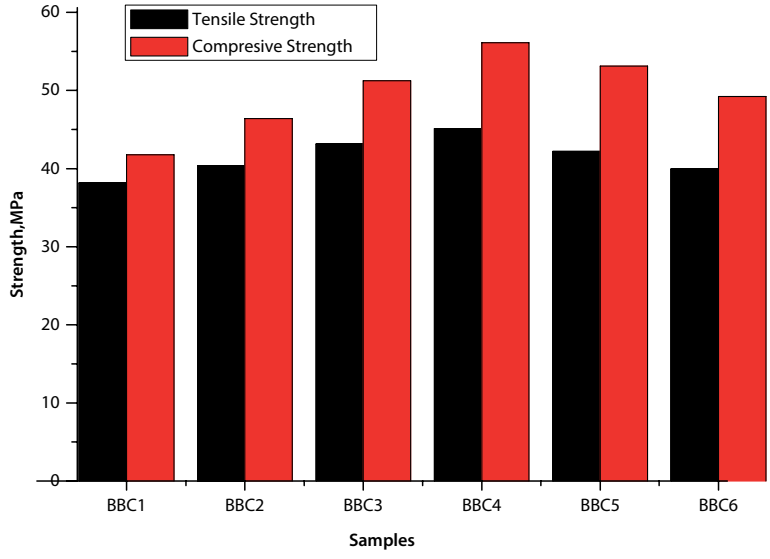

Figure 5 The tensile and compressive strengths of chitosan-g-PMMA/kaolin (BBC 1 to BBC 6).

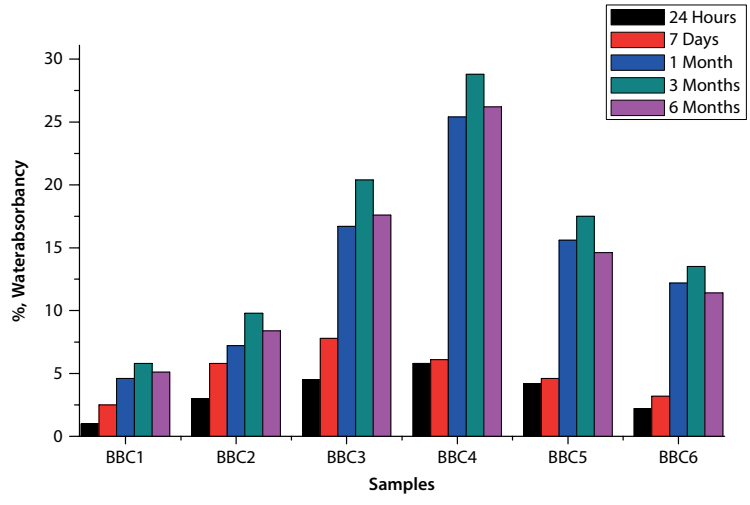

Figure 6 EWC study of chitosan-g-PMMA/kaolin (BBC1 to BBC6) BNCs.

 DOI: 10.7569/JRM.2017.634129

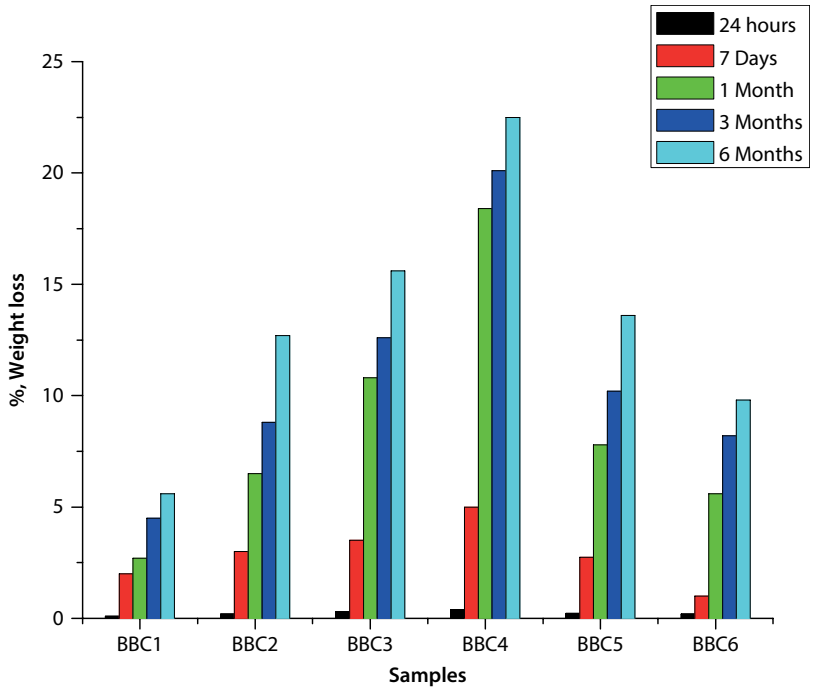

Figure 7 Biodegradation study of chitosan-g-PMMA/kaolin (BBC-1 to BBC-6) NCs.

atmosphere and were characterized by XRD, FTIR, FESEM and TGA. The grafting of PMMA onto chitosan was confirmed by FTIR as well as FESEM micrographs and the homogeneous insertion of kaolin was also confirmed from XRD and FESEM studies. The mechanical properties like tensile strength and compressive strength show similar results and the sample BBC4 was found to be more suitable BNC. The EWC was also in agreement with biodegradation results for good water retention capacity of BBC4. Finally, BNCs would be considered as an excellent material for bone substitute.

ACKNOWLEDGMENT

The authors gratefully acknowledge the financial assistance received from UGC-SAP-DSA-II, Government of India and Council of Scientific and Industrial Research (CSIR), New Delhi, India (AKP, SRF:09/173[0131]/2013-EMR-I).

REFERENCES

1. C.A. Gersbach, J.E. Phillips, and A. Garcia, Genetic engineering for skeletal regenerative medicine. *J. Annu. Rev. Biomed. Eng.* **9**, 87–119 (2007).
2. H. Xu, S.F. Othman, and R.L. Magin, Bone tissue engineering and regeneration: From discovery to the clinic—an overview. *J. Biosci. Bioeng.* **106**(6), 515–527 (2008).
3. C.T. Laurencin, A.M. Ambrosio, M.D. Borden, and J.A. Cooper Jr., Tissue engineering: Orthopedic applications. *Annu. Rev. Biomed. Eng.* **1**, 19–46 (1999).
4. A.R. Gazdag, J.M. Lane, D. Glaser, and R.A. Forster, Alternatives to autogenous bone graft: Efficacy and indications. *J. Am. Acad. Orthop. Surg.* **3**(1), 1–8 (1995).
5. F.X. Huber, N. McArthur, L. Heimann, E. Dingeldein, H. Cavey, X. Palazzi, G. Clermont, and J.P. Boutrand, Evaluation of a novel nanocrystalline hydroxyapatite paste. *BMC Musculoskelet. Disord.* **10**(164), 1–11 (2009).
6. I.O. Smith, X.H. Liu, L.A. Smith, and P.X. Ma, Nanostructured polymer scaffolds for tissue engineering and regenerative medicine. *Wiley Interdiscip. Rev. Nanomed. Nanobiotechnol.* **1**(2), 226–236 (2009).
7. R.K. Schneider, A. Puellen, R. Kramann, K. Raupach, J. Bornemann, R. Knuechel, A. Pérez-Bouza, and S. Neuss, The osteogenic differentiation of adult bone marrow and perinatal umbilical mesenchymal stem cells and matrix remodelling in three-dimensional collagen scaffolds. *Biomaterials* **31**, 467–480 (2010).
8. S. Larsson, Cement augmentation in fracture treatment. *Scand. J. Surg.* **95**, 111–118 (2006).
9. M.J. Dalby, L.D. Silvio, E.J. Harper, and W. Bonfield, Increasing hydroxyapatite incorporation into poly(methylmethacrylate) cement increases osteoblast adhesion and response. *Biomaterials* **23**(2), 569–576 (2002).
10. G. Cunin, H. Boissonnet, H. Petite, C. Blanchat, and G. Guillemin, Experimental vertebroplasty using

osteoconductive granular material. *Spine* **25**(9), 1070–1076 (2000).
11. Y.S Kim, Y.H. Kang, and J.K. Kim, Effect of bone mineral particles on the porosity of bone cement. *Biomed. Mater. Eng.* **4**(1), 37–46 (1994).
12. J.X. Lu, Z.W. Huang, and P. Tropiano, Human biological reactions at the interface between bone tissue and polymethyl methacrylate cement. *J. Mater. Sci. Mater. Med.* **13**(8), 803–809 (2002).
13. P.F. Heini, B. Walchli, and U. Berlemann, Percutaneous transpedicular vertebroplasty with PMMA operative technique and early results: A prospective study for the treatment of osteoporotic compression fractures. *Eur. Spine J.* **9**(5), 445–450 (2000).
14. J.E. Barralet, T. Gaunt, A.J. Wright, I.R. Gibson, and J.C. Knowles, Effect of porosity reduction by compaction on compressive strength and microstructure of calcium phosphatecement. *J. Biomed. Mater. Res. B Appl. Biomater.* **63**(1), 1–9 (2002).
15. A. Sogal and S.F. Hulbert, Mechanical properties of a composite bone cement: Polymethylmethacrylate and hydroxyapatite, in *Proceedings of the 5th International Symposium on Ceramics in Medicine* **5**, 213–224 (1992).
16. J.H. Dove and S.F. Hulbert, Fatigue properties of a polymethylmethacrylate-hydroxyapatite composite bone cement, in Proceedings of the 2nd International Symposium on *Apatite*, Tokyo, Japan (1995).
17. K.R. Dai, Y.K. Liu, J.B. Park, C.R. Clark, K. Nishiyama, and Z.K. Zheng, Bone-particle impregnated bone cement: An in vivo weight-bearing study. *J. Biomed. Mater. Res.* **25**, 141–156 (1991).
18. H. Onishi and Y. Machida, Biodegradation and distribution of water-soluble chitosan in mice. *Biomaterials* **20**, 175–182 (1999).
19. Y. Zhang, X. Zhang, R. Ding, J. Zhang, and J. Liu, Determination of the degree of deacetylation of chitosan by potentiometric titration preceded by enzymatic pretreatment. *Carbohydr. Polym.* **83**(2), 813–817 (2011).
20. E.J. Harper and W. Bonfield, Tensile characteristics of ten commercial acrylic bone cements. *J. Biomed. Mater. Res. B Appl. Biomater.* **53**, 605–616 (2002).
21. T.W. Federle, M.A. Barlaz, C.A. Pettigrew, K.M. Kerr, J.J. Kemper, B.A. Nuck, and L.A. Schechtman, Anaerobic biodegradation of aliphatic polyesters: Poly(3-hydroxybutyrate-co-3-hydroxyoctanoate) and poly(epsilon-caprolactone). *Biomacromolecules* **3**, 813–822 (2002).
22. G.A.F. Roberts, Chondroitin sulfate, hyaluronic acid and chitin/chitosan production using marine waste sources, in *Chitin Chemistry*, pp. 85–91, Macmillan Press Ltd., London, UK (1992).
23. J.S. Ahn, H.K. Choi, and S. Cho, A novel mucoadhesive polymer prepared by template polymerization of acrylic acid in the presence of chitosan. *Biomaterials* **22**, 923–928 (2001).
24. W.M. Cheng, G.A. Miller, J.A. Manson, R.W. Hertzberg, and L.H. Sperling, Mechanical behaviour of poly(methyl methacrylate). Part 1. Tensile strength and fracture toughness. *J. Mater. Sci.* **25**, 1917–1923 (1990).
25. Y. Lv, A. Li, F. Zhou, X. Pan, F. Liang, X. Qu, D. Qiu, and Z. Yang, A novel composite PMMA-based bone cement with reduced potential for thermal necrosis. *ACS Appl. Mater. Interfaces* **71**, 1280–11285 (2015).